J Herbmed Pharmacol. 2026; 15(2): 217-229.

http://www.herbmedpharmacol.com doi: 10.34172/jhp.2026.53362

Journal of Herbmed Pharmacology

Integrated *in silico*, *in vitro*, and *in vivo* exploration of *Nephrolepis cordifolia* for type 2 diabetes mellitus therapy

Samsul Hadi[1,2*], Deni Setiawan[1], Noer Komari[3], Askur Rahman[4], Kunti Nastiti[5], Noval[5], Hadi Kuncoro[6]

[1]Department of Pharmacy, Faculty of Mathematics and Natural Sciences, Lambung Mangkurat University, Banjarbaru, South Borneo, 70714, Indonesia
[2]Integrated Laboratory of Lambung Mangkurat University, Banjarbaru, South Borneo, 70714, Indonesia
[3]Department of Chemistry, Faculty of Mathematics and Natural Sciences, Lambung Mangkurat University, Banjarbaru, South Borneo, 70714, Indonesia
[4]Department Agricultural Industrial Technology, Faculty of Agriculture, Trunojoyo Madura University, Bankalan, East Java, 69162, Indonesia
[5]Department of Pharmacy, Faculty of Health, Sari Mulia University, Banjarmasin, South Borneo, 70127, Indonesia
[6]Department of Pharmacy, Faculty of Pharmacy, Mulawarman University, Samarinda, East Borneo, 75242, Indonesia

ARTICLE INFO

Article Type:
Original Article

Article History:
Received: 25 Aug. 2025
Revised: 3 Nov. 2025
Accepted: 23 Nov. 2025
epublished: 1 Apr. 2026

Keywords:
Hypoglycemic agents
Ethyl acetate
Ellagic acid
Molecular docking
GEO2R gene expression

ABSTRACT

Introduction: Type 2 diabetes mellitus (T2DM) is a chronic metabolic disorder characterized by insulin resistance and pancreatic β-cell dysfunction, while current pharmacological therapies often show limited efficacy and adverse side effects. *Nephrolepis cordifolia* is a traditional medicine used to treat metabolic and inflammatory diseases. This study aimed to investigate the antidiabetic potential of *N. cordifolia* through an integrative approach of *in silico*, *in vitro*, and *in vivo* to elucidate the molecular mechanisms against T2DM.

Methods: This study began with an *in vitro* assay to evaluate the ability of *N. cordifolia* to inhibit glucose release through amylolysis kinetics. *In vivo* experiments involved alloxan-induced diabetes in Wistar rats, which were administered extract doses of 200, 400, and 600 mg/kg to assess blood glucose levels and pancreatic histology. Meanwhile, *in silico* analysis identified genes expressed through GEO2R and performed molecular docking to explore potential antidiabetic mechanisms.

Results: The ethyl acetate fraction of *N. cordifolia* effectively lowered glucose levels, showing the highest glucose dialysis retardation index (GDRI) value (82.56). *In vivo* tests demonstrated that the ethanol extract significantly reduced blood glucose levels ($P < 0.05$) and improved pancreatic histology at a dose of 600 mg/kg. Gene analysis revealed involvement in the diabetic cardiomyopathy pathway, with ellagic acid as the most active compound, exhibiting strong and stable binding to mitochondrial targets, including NDUFA9 and NDUFS4.

Conclusion: *N. cordifolia* has potential as a natural product therapy candidate for the management of T2DM through specific molecular mechanisms.

Implication for health policy/practice/research/medical education:
This study implies the need to strengthen evidence-based phytopharmaceutical integration into T2DM health policies, supports the development of *Nephrolepis cordifolia* as a molecularly targeted alternative therapy, encourages further omics-based and clinical investigations, and serves as a translational research model in medical and pharmaceutical education.

Please cite this paper as: Hadi S, Setiawan D, Komari N, Rahman A, Nastiti K, Noval, et al. Integrated *in silico*, *in vitro*, and *in vivo* exploration of *Nephrolepis cordifolia* for type 2 diabetes mellitus therapy. J Herbmed Pharmacol. 2026;15(2):217-229. doi: 10.34172/jhp.2026.53362.

Introduction

Type 2 diabetes mellitus (T2DM) is a metabolic and prevalent disease that poses a serious threat to public health. According to 2023 data from the International Diabetes Federation (IDF), more than 537 million adults had diabetes, and approximately 90% suffered from T2DM (1). This disease is characterized by insulin resistance and pancreatic beta-cell dysfunction, leading to chronic hyperglycemia. In Indonesia, the prevalence of T2DM has increased significantly due to lifestyle

***Corresponding author**: Samsul Hadi,
Email: samsul.hadi@ulm.ac.id

changes, urbanization, and unhealthy diets (2). Although various pharmacological therapies are available, many patients experience complications such as nephropathy, retinopathy, and cardiovascular disease (3). This situation indicates that conventional therapies are not fully effective in controlling the disease (4). Therefore, a new method is needed that focuses not only on lowering blood glucose levels but also on the underlying molecular and genetic mechanisms. The method could open up opportunities for the development of more targeted and curative therapies, rather than solely symptomatic ones.

Several studies have identified the involvement of multiple genes in the pathogenesis of T2DM, including those that regulate insulin sensitivity, glucose metabolism, and inflammation (5). Although numerous genetic studies, such as genome-wide association studies (GWAS), have been conducted, the results still cannot fully explain the genetic variations that contribute to individual susceptibility (6). Existing literature focuses on the expression of specific genes without considering the involvement of more complex biological pathways and interactions between genes. In addition, molecular-based therapeutic methods are still limited due to a lack of understanding of differential gene expression in physiological and pathological conditions (7). Traditional medicinal plants, particularly *Nephrolepis cordifolia*, have been utilized for centuries in alternative medicine. However, the molecular potential and its associated genetic expression in plants have not been widely studied. This presents an important scientific gap that warrants exploration, particularly in the context of T2DM. Therefore, scientific studies that integrate genetic exploration with biological assays, both *in vitro* and *in vivo*, are necessary to thoroughly investigate the therapeutic potential and mechanisms of action of these plants. One plant with potential for treating DM is *N. cordifolia*.

According to previous studies, the ethanol extract of *N. cordifolia* has hepatoprotective properties, reducing liver biomarkers such as alkaline phosphatase (ALP), serum glutamic-pyruvic transaminase (SGPT), serum glutamic-oxaloacetic transaminase (SGOT), and bilirubin. It can also reduce cholesterol, triglycerides (TG), low-density lipoprotein cholesterol (LDL-C), total cholesterol (TC), and very low-density lipoprotein cholesterol (VLDL-C), while increasing catalase (CAT), superoxide dismutase (SOD), and glutathione (GSH) (8). Ethanol extract also exhibits good antibacterial and antioxidant properties, which are reinforced by active compounds detected by GC-MS, followed by docking to identify active compounds, namely methyl ester, Hexadecanoic acid, and 5-Phenyl-2,4-pyrimidinediamine (9). Studies on other species indicate that the water and methanol extracts of *Nephrolepis auriculata* possess antidiabetic properties, attributed to their flavonoid and phenolic contents (10). The ethyl acetate fraction of *N. unduranta* can lower blood sugar levels by inhibiting the hydrolysis of sugar into glucose and increasing SOD and CAT levels (11). These results were supported by *in vitro* tests on the enzymes α-amylase and α-glucosidase (12). Although several studies have reported the pharmacological benefits of *N. cordifolia*, including hepatoprotective, antioxidant, and antibacterial properties, the molecular mechanisms underlying its potential antidiabetic effects remain insufficiently elucidated. Previous investigations on related species have primarily focused on enzymatic or biochemical assays without integrating gene expression profiling or computational target prediction. This lack of integrative analysis represents a critical research gap, as the relationship between the plant's phytochemical constituents and their influence on genetic and physiological regulation in T2DM has not been clearly established. Therefore, this study aims to explore the biological activity of *N. cordifolia* in the management of T2DM through differential gene expression analysis and evaluation of its activity *in vitro* and *in vivo*. The procedures focus on identifying genes involved in the molecular pathways of T2DM pathogenesis and how active compounds from *N. cordifolia* extract can modulate these genes. By integrating *in silico*, *in vitro*, and *in vivo* approaches, this research is expected to bridge the mechanistic gap and provide comprehensive insights that support the discovery of curative and preventive medicinal plant-based interventions targeting specific genetic and molecular pathways relevant to the disease.

Materials and Methods

Equipment and materials

The materials used in this study included *N. cordifolia* tubers, Wistar rats weighing 100–150 grams, Eppendorf tubes (Onemed), vortex tubes (Jeio Tech), micropipettes (Socorex), pH meter (ACT), dialysis tubing (Carolina), Wistar rats, and a UV-Vis spectrophotometer (Perkin Elmer). Others included 96% ethanol, technical n-hexane, ethyl acetate, n-butanol, Whatman No. 1 filter paper, aluminum foil (Klinpak), distilled water, NaOH, HCl, glucose (Merck), phosphate buffer saline (PBS), starch (Merck), α-amylase enzyme (Sigma Chemical Co.), acarbose (OGB Dexa Medica), glucose oxidase peroxidase diagnostic kit (Glory® Diagnostics), and dimethyl sulfoxide (Merck).

Sample preparation

Nephrolepis cordifolia plant samples were obtained from Pemurus Baru Village, Banjarmasin (3°20′42.911″S 114°36′42.944″E) and determined in the basic laboratory of Lambung Mengkurat University with authentication number IX-24-007 and herbarium number: 173/TS-09/2024 then powdered and extracted using a maceration method with 96% ethanol for 3 × 24 hours. The extraction was carried out 3 times (one maceration and 2 remacerations) with stirring every 8 hours, then filtered and evaporated in a water bath at 55 °C to obtain a viscous

extract. Liquid-liquid fractionation was performed using graded solvents, starting with non-polar (n-hexane), semi-polar (ethyl acetate), and then polar (n-butanol), which used the partition method with a separating funnel. Each solvent was added gradually and shaken to separate the layers according to their polarity. This process was repeated until a clear fraction was obtained. All fractions formed (n-hexane, ethyl acetate, and n-butanol) were then evaporated again in a water bath at 55 °C until constant weight was achieved.

In vitro amylose kinetics test

A 4% starch solution was prepared by dissolving 4 grams of potato starch in 90 mL of 0.05 M PBS (pH 6.5). The solution was stirred at 65 °C for 30 minutes, and then it was diluted to reach a final volume of 100 mL. A total of 25 milliliters of the 4% starch solution was taken and added to 100 mg of α-amylase enzyme (0.4%) and 250 mg of *N. cordifolia* extract and fraction (1%). The mixture was then dialyzed using a dialysis tube in 200 mL of distilled water at 37 °C (pH 7.0) using a hotplate and stirrer. Positive control, used 250 mg acarbose (1%), and a control without the addition of extract or fraction samples. The absorbance of the solution was measured using a UV-Vis spectrophotometer. Furthermore, the absorbance value of the dialysate was converted to obtain the glucose content value (mg/dL) using the following formula:

$$\text{Glucose (mg/dL)} = \frac{\text{Sample absorbance}}{\text{Standard absorbance}} \times \text{Standard concentration (mg/dL)}$$

Glucose content in the dialysate was determined at 30-, 60-, 120-, and 180-minutes using glucose dialysis retardation index (GDRI), calculated according to the following formula (13):

$$\text{GDRI (\%)} = 100 - \frac{\text{Glucose content in the sample (mg/dL)}}{\text{Glucose content in control (mg/dL)}} \times 100$$

GDRI is to assess the ability of a compound, extract, or food ingredient to slow down the diffusion of glucose through a semipermeable membrane, which is used as an indicator of the potential inhibition of glucose absorption in the digestive tract.

In vivo test

The purpose of this study was to determine the ability of the extract to reduce blood glucose levels and to compare its efficacy with that of the positive control (metformin) and negative control groups. Additionally, this test aimed to determine the most effective dose of the extract that produces a significant hypoglycemic effect.

In this study, 30 test animals were divided into 6 groups, namely normal, negative control, positive control, and extract with the doses of 200, 400, and 600 mg/kg BW. The normal group received no treatment, the negative control group received 120 mg/kg of alloxan and 0.5% Na-CMC, the positive control group received 500 mg of alloxan and metformin, and the test group received 500 mg of alloxan and 3 different extract concentrations (200, 400, and 600 mg/kg). Each group consisted of 5 rats. All animals, except those in the normal group, were fasted for 16 hours and then injected intraperitoneally with alloxan (120 mg/kg body weight). The 20 test animals were monitored for 3 days after injection, followed by treatment according to the test group for 21 days. Blood samples were drawn from the test animals on day 21, and blood glucose levels were measured. Regarding the number of experimental animals, the researcher used an experimental design, using the Federer method of sample size calculation ((t−1) (r−1) ≥ 15). Data were analyzed using one-way ANOVA with a significance level of $P < 0.05$, followed by the Tukey post hoc test.

Differential gene expression *in silico*

The geodata used in this study were GSE164416, GSE25724, GSE20966, GSE76894, GSE7014, and GSE29221. The data were analyzed using GEO2R, an interactive web tool that allowed users to compare 2 or more sample groups. From this data, upregulated genes were selected, and duplicates were removed. The obtained data were then networked using STRING (https://string-db.org/). Data visualization and further analysis were performed using Cytoscape 3.10.3 software with the CytoCluster method. This analysis included closeness centrality (CC). From gene expression data, pathway analysis was performed using Enrichr (https://maayanlab.cloud/Enrichr/). In the gene expression analysis stage, data normalization was performed using the log2 transformation method to stabilize variance between samples, and *P* value correction was performed using the Benjamini–Hochberg false discovery rate (FDR < 0.05) method to minimize false positives. Differential gene selection criteria were determined based on threshold values.

Docking and pharmacophore analysis

This study used 62 previously obtained compounds (14). These compounds were subjected to pharmacophore analysis based on the similarity of glimepiride to several criteria, such as hydrogen donor (X: 4.261; Y: -2.6193; Z: 0; r: 1), hydrogen acceptor (X: 2; Y: -4.3981), hydrogen acceptor (X: 2.8941; Y: -2.6193; Z: 0), hydrophobic (X: 2.8756; Y: -6.9239; Z: 0), and hydrophobic (X: 4.8479; Y: -6.4672; Z: 0). Subsequently, drug likeness was analysed based on Lapinski's rules using SwissADME (http://www.swissadme.ch/).

Preparation of target proteins and docking procedure

Protein crystal structures downloaded from the RSCB PDB database were imported into Yasara. For molecular docking purposes, all water molecules were removed, and the protein chain corresponding to the target was selected. https://open.playmolecule.org/ was used to predict potential cavities or binding sites. Since the target protein

lacked a native ligand, the target proteins in this study were NDUFS1 (PDB ID: 8J9I, chain A), NDUFA9 (8J9I, chain L), UQCRC2 (3TGU, chain B), UQCRFS1 (8IUJ, chain MA), and NDUFS4 (8J9I, chain ZA). After obtaining the coordinates of the binding site and the compound to be tested, the next step was docking (15) using AutoDock Vina. In this process, the parameters measured included the energy values involved and the dissociation constant. Regarding the validation of the molecular docking results, we did not perform re-docking analysis using RMSD because the target proteins in this study (NDUFS1, NDUFA9, UQCRC2, UQCRFS1, and NDUFS4) did not have native ligands in their crystal structures. Therefore, validation was performed alternatively through pharmacophore fit analysis and comparison of binding energy values with a standard drug (glimepiride).

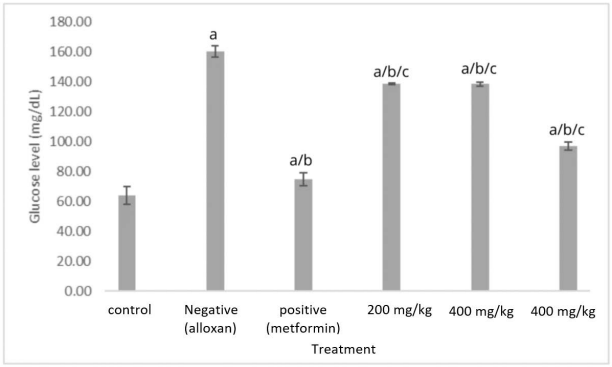

Figure 1. Effects of ethanol extract of *Nephrolepis cordifolia* in alloxan-induced Wistar rats. a: significantly different from the control; a/b: significantly different from the control and negative control; a/b/c: significantly different from the control, negative control, and positive control. Values are considered statistically significant if $P < 0.05$. The significance level was analyzed using ANOVA, followed by the Tukey test.

Results

Sample preparation

The results of the *N. cordifolia* plant determination were obtained using test number 214a/LB.LABDASAR/XI/2024. Based on the extraction, 41.64 grams of thick extract with a yield of 20.82% were obtained, comprising 2.09 grams of the n-hexane fraction (5.02%), 2.88 grams of the ethyl acetate fraction (6.94%), and 2.43 grams of the n-butanol fraction (5.88%). Subsequently, the samples were used for *in vitro* and *in vivo* tests.

In vitro amylolysis kinetics test results

In vitro test results showed that ethanol extract and *N. cordifolia* fractions could inhibit the amylolysis process, as indicated by a decrease in dissolved glucose levels over the observation period of up to 180 minutes (Table 1). Moreover, the ethyl acetate fraction showed the highest activity in inhibiting glucose release in the dialysate, at 10.22 ± 0.21 mg/dL, with the highest GDRI value closest to that of acarbose, the positive control, at 82.56 at 30 minutes. This indicated that this fraction likely contained polar active compounds such as flavonoids or tannins. The n-butanol fraction also had a significant inhibitory effect, although not as strong as the ethyl acetate fraction, with a dialysate concentration of 20.49 ± 0.53 mg/dL and a GDRI value of 71.09 at 30 minutes, indicating that semi-polar compounds contributed to the antidiabetic activity. Furthermore, the n-hexane fraction, although more nonpolar, still exhibited an inhibitory effect, suggesting the presence of lipophilic compounds. This result supported the notion that *N. cordifolia* starch digestion-inhibitory activity was influenced by the diversity of bioactive compounds in each fraction, thereby offering potential use as a natural agent for blood glucose control.

In vivo test results

In an *in vivo* test using an alloxan-induced rat model, oral administration of ethanol extract of *N. cordifolia* significantly reduced blood glucose levels compared to the negative control, particularly at the dose of 600 mg/kg, which reached 96.93 mg/dL, as shown in Figure 1. This antihyperglycemic effect suggested that the active compounds in the extract probably acted enzymatically in the gastrointestinal tract and influenced metabolic mechanisms such as pancreatic β-cell regeneration and increased insulin sensitivity, as shown in Figure 2. Doses of 200 and 400 mg/kg did not show a significant reduction, but remained lower than the negative control, indicating a gradual effect with increasing doses. The decrease in

Table 1. Effect of samples on starch digestibility and glucose dialysis retardation index (GDRI) values

Time (min)	Negative control (mg/dL)	Acarbose (mg/dL)	Ethanol extract (mg/dL)	n-Hexane fraction (mg/dL)	Ethyl acetate fraction (mg/dL)	n-Butanol fraction (mg/dL)
30	16.23±0.38	2.601 ± 0.225^{x} (83.98)	7.29 ± 0.44$^{x/y}$ (55.12)	9.64 ± 0.42$^{x/y}$ (40.61)	2.99 ± 0.17^{y} (81.56)	4.69 ± 0.22$^{x/y}$ (71.09)
60	26.22±0.36	4.911 ± 0.259^{x} (81.26)	13.32 ± 0.18 $^{x/y}$ (49.17)	20.8 ± 0.39$^{x/y}$ (20.81)	5.48 ± 0.17$^{x/y}$ (79.08)	9.16 ± 0.36$^{x/y}$ (65.03)
120	33.81±0.17	7.452 ± 0.514^{x} (77.95)	25.30 ± 0.26$^{x/y}$ (25.17)	30.4 ± 0.23$^{x/y}$ (10.01)	8.22 ± 0.23$^{x/y}$ (75.68)	14.33 ± 0.57$^{x/y}$ (57.61)
180	37.80±0.23	9.319 ± 0.262^{x} (75.35)	30.42 ± 0.29$^{x/y}$ (19.53)	36.7 ± 0.12$^{x/y}$ (2.98)	10.22 ± 0.21$^{x/y}$ (72.94)	20.49 ± 0.53$^{x/y}$ (45.81)

x: significantly different from the control; y: significantly different from the positive control; x/y: significantly different from the control and positive control. Values are considered statistically significant if $P < 0.05$. The significance level was analyzed using ANOVA, followed by the Tukey test.

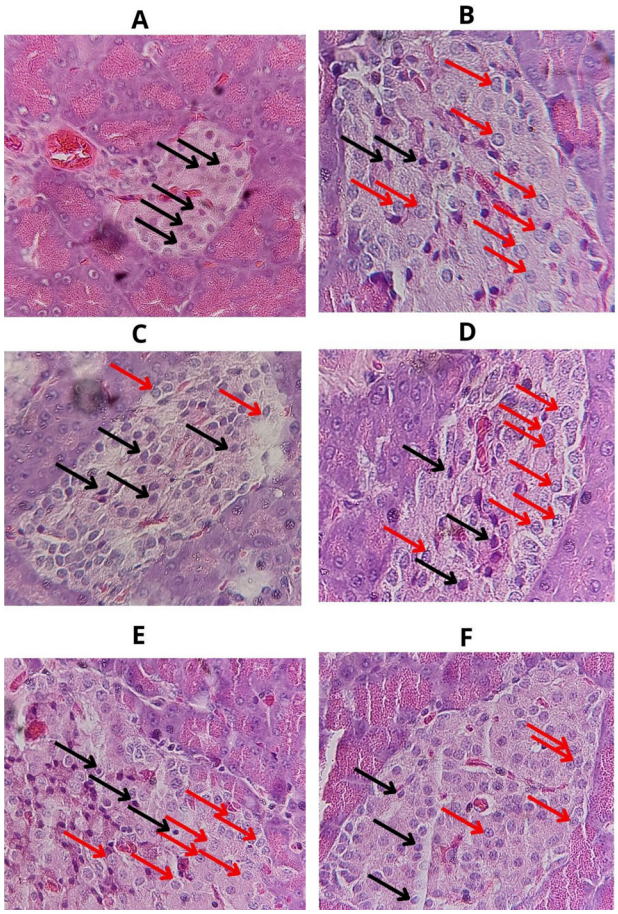

Figure 2. Histology of pancreatic tissue of Wistar rats induced by alloxan, with various treatments of ethanol extract of *Nephrolepis cordifolia*. A: normal group; B: negative control; C: positive control; D, E, and F: 200, 400, and 600 mg/kg extract groups. Red arrows: cell death; Black arrows: normal beta cells.

glucose levels at the dose of 600 mg approached the value obtained from the positive control (acarbose), indicating that the extract had promising therapeutic potential.

Observations in the normal group revealed endocrine cells dispersed in the islets of Langerhans, characterized by intact cells with a bluish-purple color and reddish cytoplasm. These results indicated that there was no cell damage in the pancreas of rats in the normal group. Microscopic observations of pancreatic tissue cells in the negative control group revealed significant cell death, while in the positive control group, cell death decreased.

Observations in the 200 mg/kg extract group showed pancreatic beta cell death, but this was already decreasing compared to the negative control group. Meanwhile, observations in the 400 mg/kg extract group showed less pancreatic beta cell damage compared to both the negative and 200 mg/kg extract groups. In the 600 mg/kg extract group, improvements in pancreatic beta cells were observed, with fewer dying compared to the negative group. Based on histopathological features of pancreatic tissue, test animals in the extract group experienced recovery from pancreatic damage caused by diabetes. This recovery was proportional to the increase in the dose of *N. cordifolia* extract.

Differential gene expression *in silico*

Based on the geodata, the normal and T2DM groups were as follows: GSE164416 (normal: 18; T2DM: 39), GSE25724 (6; 7), GSE20966 (10; 10), GSE76894 (84; 19), GSE7014 (6; 20), and GSE29221 (12; 12). The upregulated genes in GSE164416 were 1531, GSE25724 (3189), GSE20966 (20), GSE76894 (2080), GSE7014 (5342), and GSE29221 (269). Subsequently, duplicate data were removed, resulting in 7,884 data points. Based on the analysis of Figure 3 (volcano plot), significant differences in gene expression were visible between normal individuals and those with T2DM. Data from 6 GSE sets (GSE164416, GSE25724, GSE20966, GSE76894, GSE7014, and GSE29221) showed that most genes involved in T2DM were upregulated, indicating specific biological activation in response to chronic hyperglycemia. These upregulated genes likely played a role in the inflammation, oxidative stress, and metabolic dysfunction characteristic of T2DM.

The obtained data were then networked using STRING and further analyzed using Cytoscape. This process resulted in 10 main clusters: cluster 1 (Node: 61; Density; 0.787; Quality: 0.0001), cluster 2 (66; 0.486; 0.340; 0.072), cluster 3 (123; 0.501; 0.315; 0.087), cluster 3 (115; 0.476; 0.312; 0.121), cluster 4 (106; 0.500; 0.317; 0.149), cluster 5 (14; 0.923; 0.279; 0.194), cluster 6 (22; 0.519; 0.314; 0.444), cluster 7 (12; 0.515; 0.112; 0.512), cluster 8 (11; 0.673; 0.224; 0.840), cluster 9 (18; 0.601; 0.241; 0.944), and cluster 10 (25; 0.673; 0.278; 0.9). From these 10 clusters, cluster 1 was selected because it had the smallest quality value. Based on the network analysis, the node value was 61, the edge value was 144, and the average number of neighbors was 47,246. According to the cytocluster analysis, 4 groups were obtained with degree values of 57-58, 50-56, 43-49, and 10-32. This was consistent with closeness centrality (CC) values of 0.9421–0.9677, 0.8571–0.9375, 0.7792–0.8450, and 0.5357–0.6818. Furthermore, these values were comparable to radiality values of 0.9988–0.9999, 0.9971–0.9988, 0.9951–0.9968, and 0.9850–0.9919.

Figure 4 provides information on the central role of differentially expressed genes (DEGs) in the molecular interaction network based on CC values. The higher the CC value, the more significant the gene's role in the interaction network. The dominant green circle indicated genes with a very high central role (CC: 0.9421–0.9677). In Figure 5, the red V-shaped pathway is shown to have a direct involvement with the T2DM metabolic pathway, as indicated by the KEGG database. Pathways with a V-shape indicated direct involvement in the pathogenesis of diabetes. Therefore, these genes were prime candidates for further study in the development of T2DM therapies or biomarkers.

Based on pathway analysis, 10 pathways with a *P* value less than 0.05 were identified as being associated with T2DM.

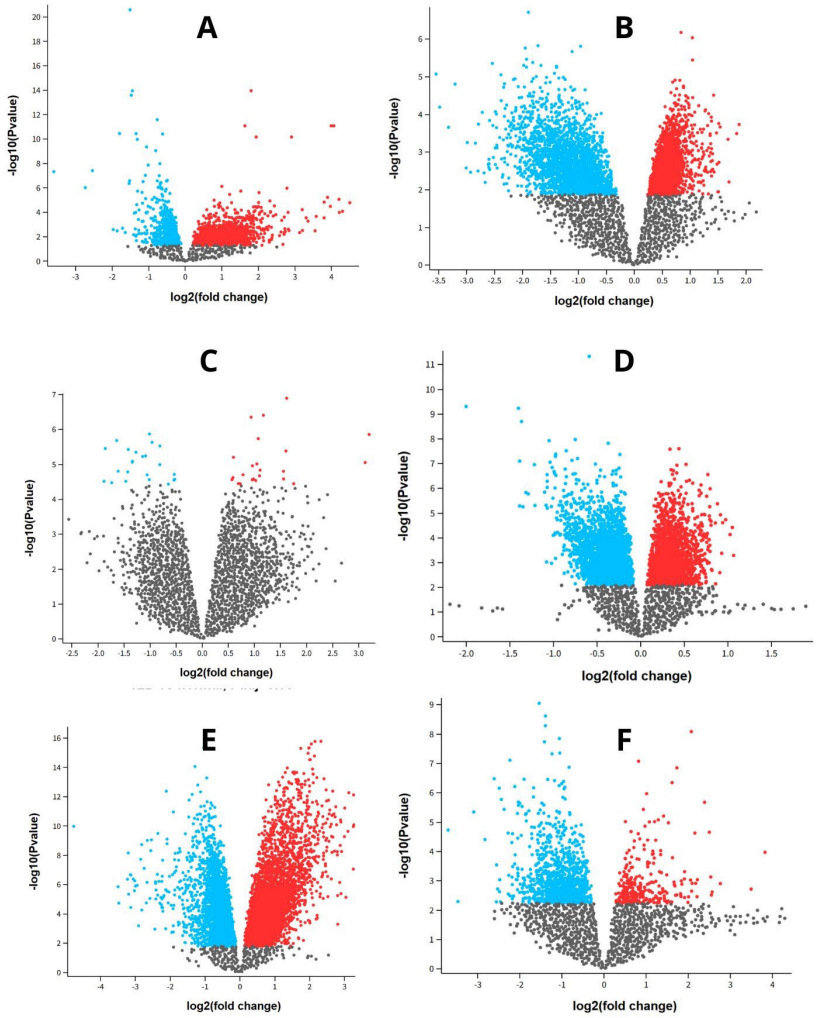

Figure 3. Volcano plot between T2D and normal conditions from GEO Browser database. *Red indicates upregulated T2D, blue indicates downregulated. A: GSE164416; B: GSE25724; C: GSE20966; D: GSE76894; E: GSE7014; F: GSE29221.

The biological pathway began with impaired oxidative phosphorylation due to mitochondrial dysfunction and increased oxidative stress in pancreatic β-cells. Thermogenesis was decreased due to insulin resistance, resulting in fat accumulation and reduced insulin sensitivity. The complications of diabetic cardiomyopathy (Figure 6) could arise from chronic hyperglycemia, which triggered oxidative stress, fibrosis, and heart cell death, making this pathway a primary target for docking analysis. The NAFLD pathway was characterized by impaired lipid and glucose metabolism, which exacerbated insulin resistance and contributed to liver complications. In cholesterol metabolism, dysregulation increased the risk of atherosclerosis through impaired HDL function and increased LDL. The ferroptosis pathway, which comprises iron-dependent cell death, also contributed to the damage of pancreatic β-cells. Cellular senescence accelerated cell damage and chronic inflammation, impairing insulin function. Necroptosis, a proinflammatory form of cell death, exacerbated pancreatic and kidney damage. Disruption of the cGMP-PKG pathway led to vascular dysfunction and metabolic disturbances. The disruption of calcium signaling reduced insulin exocytosis, with broad implications for metabolism and cardiac function.

Docking results

This analysis aimed to identify potential inhibitors that could modulate mitochondrial protein activity, particularly those contributing to impaired glucose metabolism. Based on previous studies, 62 compounds were identified, which were then screened for pharmacophore similarity to glimepiride, yielding 5 compounds: ellagic acid, hydrolyzed fumonisin B1, oleamide, stearamide, and armillaramide. The next step was drug-likeness screening based on Lapinkiy's rule. Armillaramide was excluded due to its MW >500 and MLOGP >4.15, resulting in 555.5217 and 4.98, respectively, as presented in Table 2.

The docking analysis results showed that ellagic acid had the highest affinity for the 5 target genes in the pathogenesis of T2DM, including NDUFS1, NDUFA9, UQCRC2, UQCRFS1, and NDUFS4 (Figure 7). For the NDUFA9 gene, ellagic acid performed the best

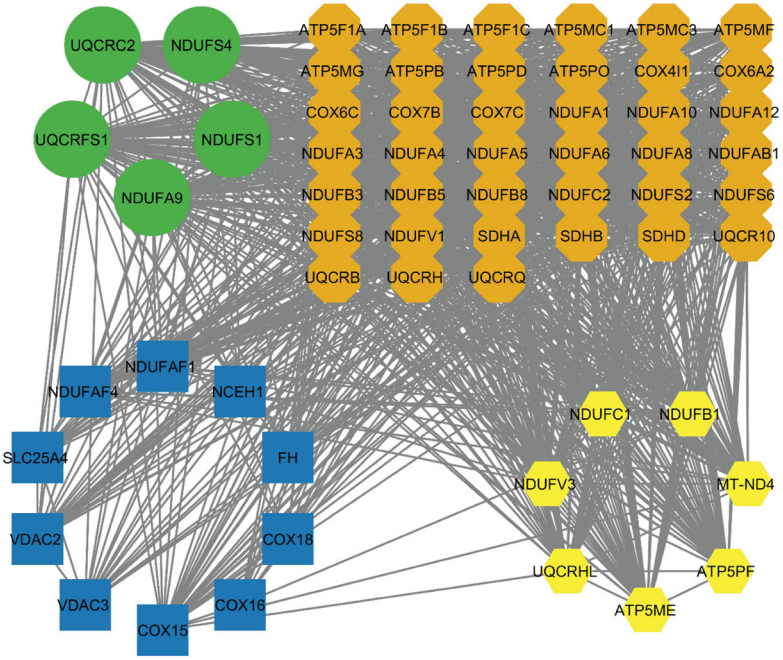

Figure 4. Up-regulated DEG (differentially expressed genes) interaction network in general. Green circle with closeness centrality (CC) values: 0.9421-0.9677; brown octagon with CC values: 0.8571-0.9375; yellow hexagon with CC values: 0.7792-0.8450; blue rectangle with CC values: 0.5357-0.6818.

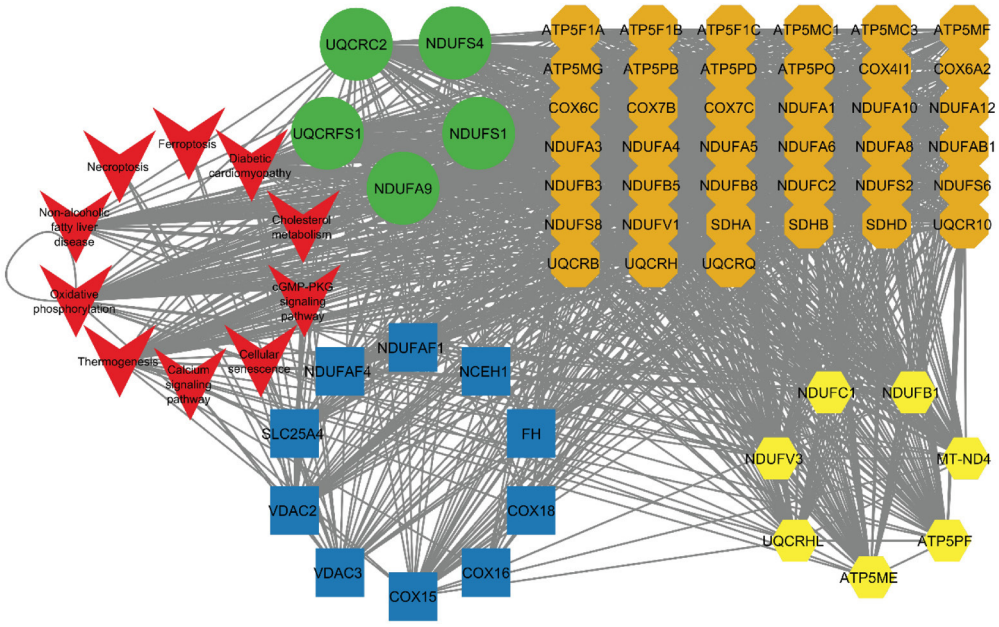

Figure 5. General up-regulated DEG (differentially expressed genes) interaction network associated with the Kegg pathway for type 2 diabetes mellitus (T2DM). Green circle with closeness centrality (CC) values: 0.9421 - 0.9677; brown octagon with CC values: 0.8571-0.9375; yellow hexagon with CC values: 0.7792-0.8450; blue rectangle with CC values: 0.5357-0.6818; red V: Kegg pathway for T2DM.

with a binding energy (BE) of -9.882 kcal/mol and a dissociation constant (DC) of 57.068 μM, indicating a robust and stable bond. Interactions with key residues such as ARG148, ARG161, and TYR180 strengthened its potential inhibitory activity on mitochondrial complex I. Furthermore, ellagic acid exhibited a high affinity for NDUFS4 (BE -9.056 kcal/mol; DC 230.072 μM), with the involvement of positively charged residues, such as ARG68, ARG70, ARG83, and ARG115, supporting strong electrostatic and polar interactions.

For other targets, such as NDUFS1 and UQCRC2, ellagic acid continued to exhibit a competitive affinity with BEs of -8.874 and -8.75 kcal/mol, respectively, and DCs below 400,000 μM, which was much lower than that

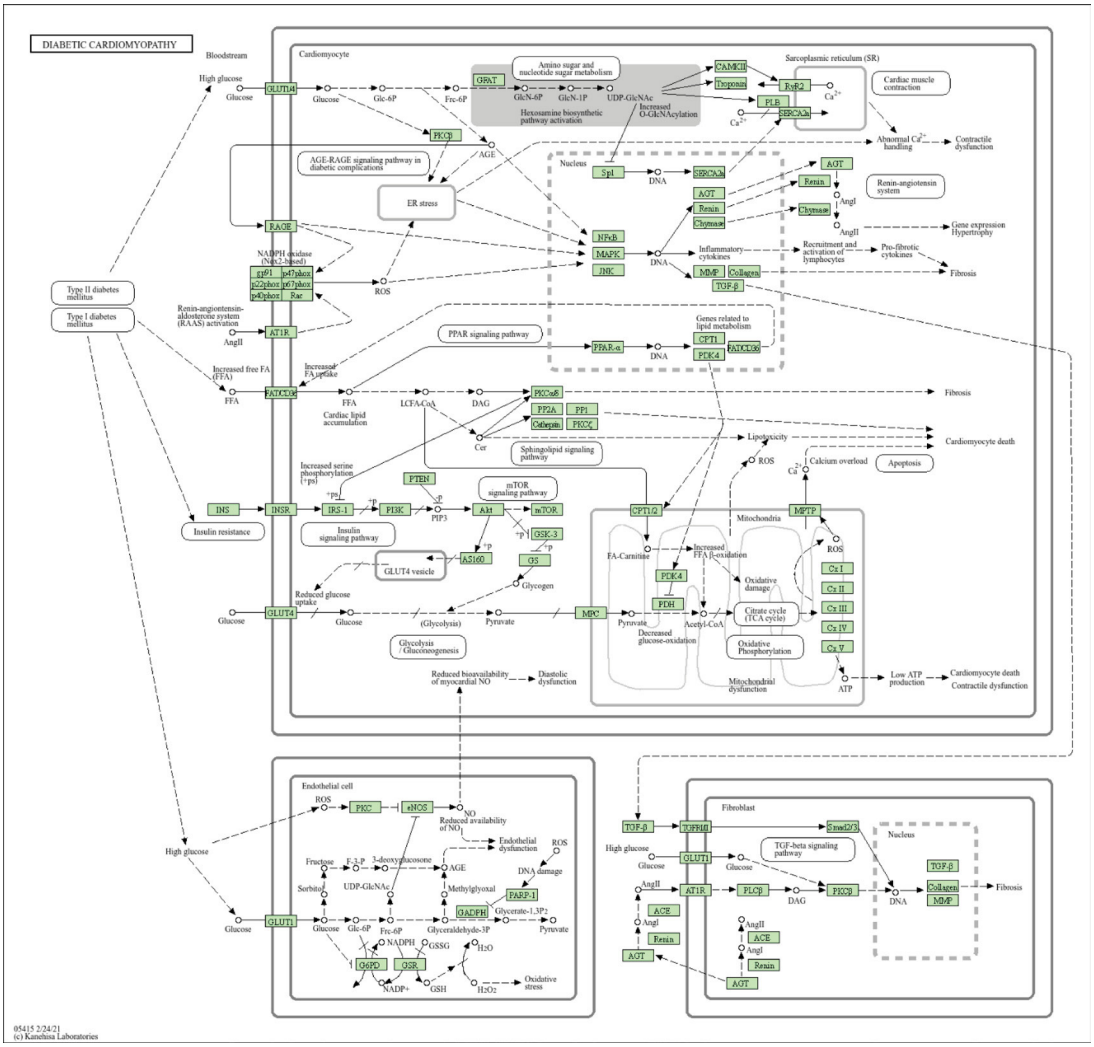

Figure 6. Genes from DEGs (differentially expressed genes) obtained from 6 geobrowsers and involved in diabetic cardiomyopathy.

of other compounds. This indicated that the interactions formed were stable, primarily through aromatic and polar residues such as HIS194 and ILE193, as well as hydrogen bonds with ASN137 and ILE193 (NDUFS1), and electrostatic interactions with LYS104, and hydrogen bonds with SER384 (UQCRC2). The weakest bond of ellagic acid with UQCRFS1 had a BE value of -7.545 and DC 2947417, but this value was better than the other 3 ligands. Hydrolyzed fumonisin B1, Oleamide, and Stearamide showed less negative binding energy and tremendous DC values, reaching tens to hundreds of millions of pM, indicating weak and unstable bonds. This indicated that the 3 compounds were less effective as inhibitors of mitochondrial proteins involved in glucose metabolism, as shown in Table 3. Although the docking results indicate that ellagic acid exhibits a fairly low binding energy value, suggesting a strong affinity for the receptor, its strength is still weaker compared to the standard drug, glimepiride. This can be seen from the comparison of binding energy values, which show that the more negative the energy value, the stronger the binding affinity. Based on the data, the binding energy of ellagic acid to several protein targets was recorded as higher than glimepiride, namely on NDUFS1 (-8.874 vs -8.929),

Table 2. Physical and chemical properties of selected compounds from *Nephrolepis cordifolia* that met pharmacophore selection and Lipinski's rule

Name	Calc. MW	H aceptor	H donor	TPSA	MLog
Ellagic acid	302.0059	8	4	141.34	0.951
Hydrolyzed fumonisin B1	405.3446	7	2	99.05	-1.735
Oleamide	281.2716	2	2	44.08	4.57
Stearamide	283.2874	2	2	44.08	4.67

MW: Molecular weight; TPSA: Topological polar surface area.

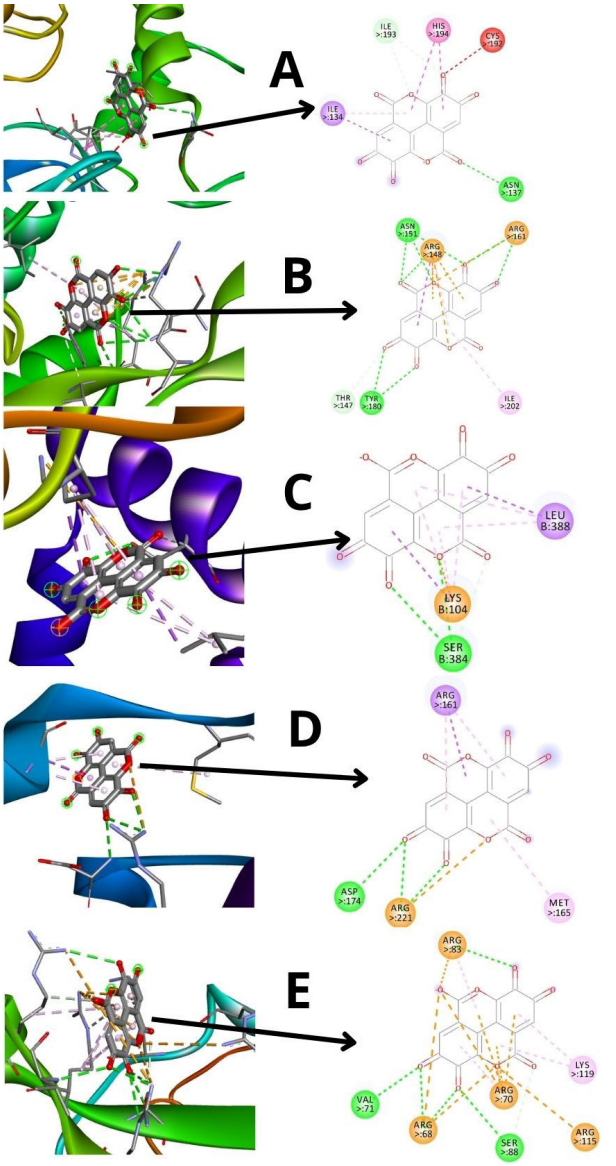

Figure 7. Interaction between protein and ellagic acid. Left: 3 dimensions; right: 2 dimensions. A: NDUFS1; B: NDUFA9; C: UQCRC2; D: UQCRFS1; E: NDUFS4.

NDUFA9 (-9.882 vs -9.969), UQCRC2 (-8.75 vs -9.225), UQCRFS1 (-7.545 vs -7.776), and NDUFS4 (-9.056 vs -9.258). These findings indicate that although ellagic acid has good interaction potential, glimepiride still shows a stronger affinity for all tested receptors.

Discussion

The *in vivo* tests demonstrated a reduction in pancreatic beta cell death induced by alloxan at a dose of 600 mg/kg body weight, as well as a positive control (metformin). This was due to the effect of metformin on reducing peripheral blood glucose (16). Furthermore, metformin has been shown to reduce pancreatic beta cell death (17). Other studies have demonstrated protective effects on various organs, including the heart and cardiovascular system (18). In vitro studies of kinetic amylosis from aqueous extracts of *Lagenaria siceraria* showed 0.32 ± 0.01, *Cynodon dactylon* 0.34 ± 0.01, and *Stevia rebaudiana* 0.31 ± 0.01(19). Ripe *Musa sapientum* was 0.41 ± 0.01(19), *M. koenigii* was 0.37 ± 0.01, and *C. roseus* was 0.40 ± 0.01 (20). In the alloxan-induced *in vivo* test, the chlorophorome fraction of *Nelsonia canescens* 300 mg/kg could reduce glucose levels to 119.00±2.70 mg/dL (21), methanol extract of *Tephrosia pumila* at a dose of 400 mg/kg was able to reduce blood sugar levels to 143.5±2.717 mg/dL (22), at a dose of 500 mg/kg, methanol extract of *Thymus schimperi* was able to reduce it to 195.5±13.1 mg/dL (23). With streptozotocin induction, a Thai herbal formula at a dose of 250 mg/kg body weight was found to reduce HbA1c and blood glucose levels (24). *Lepisanthes rubiginosa* (Roxb.) Leenh leaf and pericarp extract, administered at a dose of 500 mg/kg body weight, effectively decreased blood glucose levels by restoring pancreatic histopathology (25). T2DM could be divided into several phenotypes based on the level of insulin resistance, impaired beta-cell function, and response to therapy (5). Furthermore, accompanying complications were classified into acute complications, including hyperosmolar as well as hyperglycemia, and chronic complications, such as microvascular and macrovascular damage (26). At the molecular level, impaired insulin signaling pathways, oxidative stress, and chronic inflammation contributed to disease progression (27). Elevated levels of proinflammatory cytokines such as TNF-α and IL-6, as well as mitochondrial dysfunction, also contributed to insulin resistance and cell damage (28). Therefore, classifying T2DM based on its biological characteristics opened up opportunities for more specific therapies, including pharmacogenomic methods or plant-based therapies with targeted molecular mechanisms (29).

Differential gene expression could be categorized based on the direction of expression changes, namely upregulation (increased expression) and downregulation (decreased expression) (30). These changes indicated a cell's response to environmental stress, chemical stimuli, or specific pathological conditions. In modern genetic studies, identifying DEGs was often the initial step in determining disease biomarkers, understanding drug mechanisms of action, or evaluating the effects of therapeutic agents (31). Furthermore, the manifestations of differential gene expression varied widely, depending on tissue type and disease stage. In patients with T2DM, there was decreased expression of insulin receptor substrate (IRS) genes, as well as increased expression of inflammatory genes such as NF-κB (32). Other categories of differential expression included cellular signaling pathways, such as the PI3K-Akt and AMPK pathways, which contributed to energy metabolism and insulin response, respectively (33). Comprehensive differential gene expression analysis also allowed data integration with bioinformatics to map gene network interactions, providing a comprehensive picture of the molecular mechanisms.

Table 3. Docking results for the top five target proteins involved in the diabetic cardiomyopathy pathway

Protein target	Docking parameters and interaction types	Compound				
		Glimepiride (standard)	Ellagic acid	Hydrolyzed fumonisin B1	Oleamide	Stearamide
NDUFS1 (PDB: 8J9I)	Binding energy [kcal/mol]	-8.929	-8.874	-6.601	-5.644	-5.914
	Dissociation constant [pM]	272997	312803	14501163	72927808	46236028
	Hydrogen bond	PHE133	ASN137; ILE193	ASN190; ILE193; CYS89; CYS192; HIS194	HIS174	HIS174; ASP220; PRO221
	Hydrophobic	HIS194; PRO221; PHE133; HIS174; HIS194; ILE134	ILE134; HIS194	PHE133; ILE130; ILE134; ILE193; PRO176; HIS174; HIS194	PHE133; ILE130; ILE134; ILE193; HIS174; HIS194	PRO221; ILE130; ILE134; ILE193; HIS174; HIS194
	Electrostatic	HIS194	-	-	-	-
NDUFA9 (PDB: 8J9I)	Binding energy [kcal/mol]	-9.969	-9.882	-7.092	-6.972	-6.593
	Dissociation constant [pM]	49274	57068	6331332	7752758	14698294
	Hydrogen bond	TYR180	ARG148; ASN151; ARG161; TYR180; THR147	ASN151; TYR180; ASN125	ASN125	-
	Hydrophobic	LEU220; PHE215; ARG161; PHE163	ARG148; ILE202	ARG148; PRO182; ILE202; LEU220	ARG148; ARG161; PRO182; LEU220; ILE202; TYR180; PHE215	ARG148; ARG161; PRO182; ILE202; LEU220; PHE215
	Electrostatic	ARG148; ARG161	ARG148; ARG161	-	-	-
UQCRC2 (PDB: 3TGU)	Binding energy [kcal/mol]	-9.225	-8.75	-7.246	-6.406	-6.197
	Dissociation constant [pM]	172975	385624	4882155	20153002	28677334
	Hydrogen bond	ASN380; GLU103; ASN315	SER384	GLU103; SER317; ASN315; LYS52	GLU103	1
	Hydrophobic	LEU388; LYS104; LEU387; LYS52	LYS104; LEU388; LYS104	LYS104; LEU388; TYR316	LYS52; LYS104; VAL264; LEU388	LYS104; VAL264; LEU388; LEU387
	Electrostatic	GLU103; GLU381	LYS104	-	-	-
UQCRFS1 (PDB: 8IUJI)	Binding energy [kcal/mol]	-7.776	-7.545	-6.23	-5.381	-5.193
	Dissociation constant [pM]	2504639	2947417	27123732	113677552	156127904
	Hydrogen bond	ARG161; ALA162; VAL163	ASP174; ARG221	MET165; ARG221; PRO164; VAL163; MET160; GLU175	ASP174; ARG221; MET160; VAL163	ASP174; ARG221; MET160
	Hydrophobic	ARG161; MET165; PRO164	ARG161; MET165	PRO164	ARG161; ALA162; PRO164; MET165	ARG161; ALA162; MET165
	Electrostatic	GLU175; ARG161	ARG221	-	-	-
NDUFS4 (8J9I)	Binding energy [kcal/mol]	-9.258	-9.056	-5.381	-5.185	-5.29
	Dissociation constant [pM]	184719	230072	113677552	158250320	132549648
	Hydrogen bond	ARG68; VAL71; ARG83; SER88; ARG70	ARG68; VAL71; ARG83; SER88; ARG70	ARG68; ARG115; VAL71; HIS90; VAL71	ARG70; LYS119	ARG70; ARG116
	Hydrophobic	ARG70; LYS119	ARG70; LYS119; ARG83	ARG70; ARG83; ARG115; ARG116; LYS119; VAL71; HIS90	ARG70; VAL71; ARG83; ARG116; LYS119; HIS90	ARG70; ARG115; ARG116; LYS119; VAL71; HIS90
	Electrostatic	ARG68; HIS90	ARG68; ARG70; ARG83; ARG115	-	-	-

Binding energy: Between the ligand and the receptor; Dissociation constant shows the strength of the ligand's affinity for the receptor in the form of a concentration value.

The integration of gene expression analysis and pharmacological effects provides a more comprehensive understanding of the molecular mechanisms underlying the antidiabetic activity of *N. cordifolia*. The gene expression analysis revealing the involvement of the diabetic cardiomyopathy pathway strengthens the evidence that active compounds such as ellagic acid, together with hydrolyzed fumonisin B1, oleamide, and stearamide, play crucial roles in ameliorating mitochondrial dysfunction and oxidative stress—two major contributing factors in T2DM (34). This finding is consistent with the *in vivo* results, which demonstrated pancreatic histological improvement and a reduction in blood glucose levels in treated rats, indicating that modulation of genes associated with mitochondrial function directly contributes to β-cell recovery and enhanced insulin sensitivity. Thus, the relationship between gene expression changes and physiological outcomes confirms that the pharmacological effects of *N. cordifolia* are not merely symptomatic but are rooted in specific molecular mechanisms targeting cellular energy regulation and glucose metabolism (35).

At the molecular level, T2DM is a complex metabolic disorder characterized by insulin resistance, β-cell dysfunction, chronic inflammation, and oxidative stress, which are primarily induced by impaired mitochondrial oxidative phosphorylation, particularly within Complex I (5). The disruption of OXPHOS and inflammatory signaling contributes significantly to the pathogenesis of T2DM, highlighting the intricate interactions among inflammation, oxidative stress, and insulin resistance (27). In the present study, the gene expression profile revealed the involvement of NDUFA9 and NDUFS4 as key subunits of Complex I, which play critical roles in energy production and the regulation of reactive oxygen species (ROS) levels (36).

Furthermore, although the *in silico* results indicate that ellagic acid is the most potent compound with the highest affinity toward mitochondrial protein targets, the overall antidiabetic activity of *N. cordifolia* is likely the result of synergistic interactions among multiple phytochemicals within the extract. Other compounds, including hydrolyzed fumonisin B1, oleamide, and stearamide, may act complementarily to enhance metabolic pathway modulation, stabilize protein–ligand interactions, and reduce oxidative stress associated with insulin resistance. These synergistic phytoconstituent effects enable multi-target mechanisms that contribute to overall metabolic homeostasis rather than relying solely on single enzymatic inhibition. Therefore, the combination of active compounds in *N. cordifolia* may provide a broader and more sustainable therapeutic effect, reinforcing its potential role as an adjuvant therapy candidate for T2DM. However, limitations of this study lie in the lack of further validation of gene expression and the toxicity of this plant extract. Therefore, future studies should focus on *in vitro* and *in vivo* validation of gene expression data, as well as comprehensive toxicity and pharmacokinetic evaluations to ensure the safety and efficacy of the proposed compound.

Conclusion

In conclusion, *N. cordifolia*, particularly the ethyl acetate fraction, exhibits significant antidiabetic activity *in vitro*, and ethanol extract *in vivo* can repair alloxan-induced pancreatic beta cell damage in rats. This activity is supported by differential gene expression analysis and molecular docking, which identify ellagic acid as a strong candidate for inhibiting mitochondrial proteins involved in the diabetic cardiomyopathy pathway in T2DM. However, limitations of this study lie in the lack of further validation of gene expression and the toxicity of this plant extract.

Acknowledgement

We would like to thank to Lambung Mangkurat University for providing facilities for this research.

Authors' contribution

Conceptualization: Samsul Hadi.
Data curation: Noer Komari.
Formal analysis: Samsul Hadi.
Funding acquisition: Samsul Hadi.
Investigation: Noer Komari.
Supervision: Hadi Kuncoro.
Validation: Kunti Nastiti.
Visualization: Askur Rahman.
Writing–original draft: Noval.
Writing–review & editing: Deni Setiawan.

Conflict of interests

The authors declare no conflict of interest in this study.

Ethical considerations

The research protocol has been approved by the Research Ethics Commission of Sari Mulia University, Banjarmasin, Indonesia (No. 391/KEP-UNISM/VII/2024).

Funding/Support

This study was supported by a competitive grant from Lambung Mangkurat University (Grant number: 1885/UN8.2/PG/2025).

References

1. Hossain MJ, Al-Mamun M, Islam MR. Diabetes mellitus, the fastest growing global public health concern: Early detection should be focused. Health Sci Rep. 2024;7(3):2000-2004. doi: 10.1002/hsr2.2004.
2. Wu Y, Ding Y, Tanaka Y, Zhang W. Risk factors contributing to type 2 diabetes and recent advances in the treatment and prevention. Int J Med Sci. 2014;11(11):1185–200. doi: 10.7150/ijms.10001.
3. Sugandh F, Chandio M, Raveena F, Kumar L, Karishma F, Khuwaja S, et al. Advances in the management of diabetes

mellitus: A focus on personalized medicine. Cureus. 2023;15(8):1-13. doi: 10.7759/cureus.43697.
4. Husna F, Marisa M, Suryawati S, Suyatna FD, Husnah H, Hakim RW, et al. Traditional remedies from Aceh for diabetes mellitus treatment: Patterns of use in rural-urban areas in Aceh. Clin Epidemiol Glob Heal. 2025;34:1020-1079. doi: 10.1016/j.cegh.2025.102079.
5. Galicia-Garcia U, Benito-Vicente A, Jebari S, Larrea-Sebal A, Siddiqi H, Uribe KB, et al. Pathophysiology of type 2 diabetes mellitus. Int J Mol Sci. 2020;21(17):1-34. doi: 10.3390/ijms21176275.
6. Uffelmann E, Huang QQ, Munung NS, de Vries J, Okada Y, Martin AR, et al. Genome-wide association studies. Nat Rev Methods Prim. 2021;1(1):1-59. doi: 10.1038/s43586-021-00056-9.
7. Stanford BCM, Clake DJ, Morris MRJ, Rogers SM. The power and limitations of gene expression pathway analyses toward predicting population response to environmental stressors. Evol Appl. 2020;13(6):1166-82. doi: 10.1111/eva.12935.
8. Rajeshekar U, Swamy BM, Jayaveera KN. Hepatoprotective activity of hydro-alcoholic extract of whole plant of *Solanum dulcamara* L. and *Nephrolepis cordifolia* (L) C. Presl against paracetamol induce hepatotoxicity in albino rats. Asian J Pharm Clin Res. 2015;1(8):364–370.
9. Manimegalai P, Selvam K, Prakash P, Kirubakaran D, Shivakumar M, SenthilNathan S. In-vitro antibacterial, antioxidant and anti-inflammatory and In-silico ADMET, molecular docking study on *Hardwickia binata* phytocompunds with potential inhibitor of skin cancer protein. Silico Pharmacol. 2023;11(25):1-19. doi: 10.1007/s40203-023-00163-3. doi: 10.1007/s40203-023-00163-3.
10. Sureshkumar J, Ayyanar M. Phytochemical Composition and In Vitro Antioxidant and Antidiabetic Activities of *Nephrolepis auriculata* (L.) Trimen: An Unexplored Ethnomedicinal Fern BT - Ferns: Biotechnology, Propagation, Medicinal Uses and Environmental Regulation. In: Marimuthu J, Fernández H, Kumar A, Thangaiah S, eds. Springer Nature; 2022. 571–584. doi: 10.1007/978-981-16-6170-9_24.
11. Ojieh AE. Evaluation of antidiabetic and antioxidant potential of *Nephrolepis unduranta* leaf extract in streptozotocin induced diabetic Wistar rats. Int J Forensic Med Invest. 2020;5(1):34–41.
12. Ossai N, Richard, Anthony E, Nwogueze BC, Olowe G, Eyituoyo A. Ameliorative potentials of methanolic leaf extract of *Nephrolepis undulate* in streptozotocin-induced diabetic Wistar rats. Plant Cell Biotechnol Mol Biol. 2021;1(22):41–53.
13. Bhinge SD, Bhutkar MA, Randive DS, Wadkar GH, Hasabe TS. In vitro hypoglycemic effects of unripe and ripe fruits of *Musa sapientum*. Brazilian J Pharm Sci. 2017;53(4):1–6. doi: 10.1590/s2175-97902017000400159.
14. Hadi S, Setiawan D, Komari N, Rahmadi A, Rahman A, Fansuri H, et al. Network pharmacology and docking of *Nephrolepis cordifolia* as type-2 antidiabetic agent. Trop J Nat Prod Res. 2024;8(9). doi: 10.26538/tjnpr/v8i9.16.
15. Gaballah S, Amer H, Hofinger-Horvath A, Al-Moghazy M, Hemida M. Synthesis, antimicrobial, and docking investigations of remarkably modified sulfathiazole derivatives. Egypt J Chem. 2019;63(1):171-184. doi: 10.21608/ejchem.2019.13909.1862.
16. Huang H, Lorenz BR, Zelmanovitz PH, Chan CB. Metformin preserves β-Cell compensation in insulin secretion and mass expansion in prediabetic Nile rats. Int J Mol Sci. 2021;22(1):421-435. doi: 10.3390/ijms22010421.
17. He X, Gao F, Hou J, Li T, Tan J, Wang C, et al. Metformin inhibits MAPK signaling and rescues pancreatic aquaporin 7 expression to induce insulin secretion in type 2 diabetes mellitus. J Biol Chem. 2021;297(2):1-11. doi: 10.1016/j.jbc.2021.101002.
18. Bu Y, Peng M, Tang X, Xu X, Wu Y, Chen AF, et al. Protective effects of metformin in various cardiovascular diseases: Clinical evidence and AMPK-dependent mechanisms. J Cell Mol Med. 2022;26(19):4886–903. doi: 10.1016/j.jbc.2021.101002.
19. Randive D, Bhutkar M, Bhinge S, Shejawal K, Sanap P, Patil P, et al. Hypoglycemic effects of *Lagenaria siceraria, Cynodon dactylon* and *Stevia rebaudiana* extracts. J Herbmed Pharmacol. 2019;8:51–55. doi: 10.15171/jhp.2019.09.
20. Bhutkar M. Studies on glucose adsorption capacity of some indigenous plants. Glob J Pharm Pharm Sci. 2018;5(1):1–4. doi: 10.19080/gjpps.2018.05.555651.
21. Daniel AI, Gara TY, Ibrahim YO, Muhammad FM, Salisu FE, Tsado R, et al. In vivo antidiabetic and antioxidant activities of chloroform fraction of *Nelsonia canescens* leaf in alloxan-induced diabetic rats. Pharmacol Res Mod Chinese Med. 2022;3(1):1-7. doi: 10.1016/j.prmcm.2022.100106.
22. Ramesh C, Rani AP. In vivo and in vitro antidiabetic potentials of methanol extract of *Tephrosia pumila* against alloxan-induced diabetes in experimental animals. Int J Health Sci (Qassim). 2019;13(3):10–8.
23. Melesie Taye G, Bule M, Alemayehu Gadisa D, Teka F, Abula T. In vivo Antidiabetic Activity Evaluation of Aqueous and 80% Methanolic Extracts of Leaves of *Thymus schimperi* (Lamiaceae) in Alloxan-induced Diabetic Mice. Diabetes Metab Syndr Obes. 2020;13(1):3205–3212. doi: 10.2147/DMSO.S268689.
24. Katisart T, Butkhup L, Sumalee A, Taepongsorat L, Konsue A. Antidiabetic potential of seven-herb Thai formula: Effect on blood glucose, lipid profile, and pancreatic islet restoration in diabetic rats. Trop J Pharm Res. 2025;24(2):203–212. doi: 10.4314/tjpr.v24i2.8
25. Konsue A, Butiman C, Luang-In V, Maneechai S, Katisart T. Anti-hyperglycemic activities of *Lepisanthes rubiginosa* (Roxb.) Leenh. leaf and pericarp extracts in streptozotocin-induced diabetic rats. Trop J Pharm Res. 2024;23(12):2035–41. doi: 10.4314/tjpr.v23i12.8.
26. Banday MZ, Sameer AS, Nissar S. Pathophysiology of diabetes: An overview. Avicenna J Med. 2020;10(4):174–88. doi: 10.4103/ajm.ajm_53_20.
27. Verdile G, Keane KN, Cruzat VF, Medic S, Sabale M, Rowles J, et al. Inflammation and oxidative stress: the molecular connectivity between insulin resistance, obesity, and Alzheimer's disease. Mediators Inflamm. 2015;2015:105828. doi: 10.1155/2015/105828.
28. Berbudi A, Khairani S, Tjahjadi AI. Interplay between insulin resistance and immune dysregulation in type 2 diabetes mellitus: implications for therapeutic interventions. ImmunoTargets Ther. 2025;14:359–82. doi: 10.2147/ITT.S499605
29. Iheagwam FN, Iheagwam OT. Diabetes mellitus: The pathophysiology as a canvas for management elucidation and strategies. Med Nov Technol Devices. 2025;25:100351. doi: 10.1016/j.medntd.2025.100351.
30. Kedlian VR, Donertas HM, Thornton JM. The widespread

increase in inter-individual variability of gene expression in the human brain with age. Aging. 2019;11(8):2253-80. doi: 10.18632/aging.101912.
31. Babu G, Nobel FA. Identification of differentially expressed genes and their major pathways among the patient with COVID-19, cystic fibrosis, and chronic kidney disease. Informatics Med Unlocked. 2022;32:101038. doi: 10.1016/j.imu.2022.101038.
32. Hameed I, Masoodi SR, Mir SA, Nabi M, Ghazanfar K, Ganai BA. Type 2 diabetes mellitus: From a metabolic disorder to an inflammatory condition. World J Diabetes. 2015 ;6(4):598–612. doi: 10.4239/wjd.v6.i4.598.
33. Huang X, Liu G, Guo J, Su Z. The PI3K/AKT pathway in obesity and type 2 diabetes. Int J Biol Sci. 2018;14(11):1483–96. doi: 10.7150/ijbs.27173.
34. Yousef H, Khandoker AH, Feng SF, Helf C, Jelinek HF. Inflammation, oxidative stress and mitochondrial dysfunction in the progression of type II diabetes mellitus with coexisting hypertension. Front Endocrinol. 2023;14(1):1173402–1173412. doi: 10.3389/fendo.2023.1173402.
35. Rani R, Chitme HR, Kukreti N, Pant P, Abdel-Wahab BA, Khateeb MM, et al. Regulation of insulin resistance, lipid profile and glucose metabolism associated with polycystic ovary syndrome by *Tinospora cordifolia*. Nutrients. 2023;15:1-23. doi: 10.3390/nu15102238.
36. Kahlhöfer F, Gansen M, Zickermann V. Accessory subunits of the matrix arm of mitochondrial complex i with a focus on subunit NDUFS4 and its role in complex I function and assembly. Life. 2021;11(5):455–68. doi: 10.3390/life11050455.